

Antifungal Activity of Amphotericin B Conjugated to Carbon Nanotubes

Monica Benincasa,[†] Sabrina Pacor,[†] Wei Wu,^{*,‡} Maurizio Prato,^{§,*} Alberto Bianco,^{*,*§} and Renato Gennaro^{†,*}

[†]Department of Life Sciences, University of Trieste, Italy, [‡]CNRS, Institut de Biologie Moléculaire et Cellulaire, Laboratoire d'Immunologie et Chimie Thérapeutiques, Strasbourg, France, and [§]Department of Pharmaceutical Sciences, University of Trieste, Italy. [‡]Current address: Laboratory of Mesoscopic Chemistry and Department of Polymer Science & Engineering, College of Chemistry & Chemical Engineering, Nanjing University, People's Republic of China.

Opportunistic fungal infections are a major problem for public health. The increased number of immunocompromised patients associated with the advent of AIDS, with the increase in the frequency of solid organ and hematopoietic stem cell transplants and with more aggressive chemotherapy has led to a dramatic rise in the incidence of systemic mycoses. Amphotericin B (AMB) is considered the first-line therapy for systemic fungal infections because of its broad-spectrum antifungal activity. For over 50 years, AMB deoxycholate (AMBD), the conventional colloidal dispersion formulation known as Fungizone, has been the treatment of choice for these infections, despite its association with significantly high adverse effects,^{1,2} notably severe nephrotoxicity.³ One reason for this toxicity is the formation of aggregates as a result of its low water solubility.⁴

Improved treatment options for invasive fungal infections have been developed during the last 15 years. These involve both new antifungal agents, such as triazoles and the echinocandins, and less toxic lipid formulations of AMB, which have been added to the arsenal available against fungal infections. Some of the new drugs can now replace AMBD as primary therapy, for example, caspofungin for candidiasis⁵ and voriconazole for aspergillosis,^{6–10} while others offer therapeutic options for difficult-to-treat infections, such as posaconazole for zygomycosis,^{11–13} fusariosis^{14,15} and chromoblastomycosis.¹⁶ However, the extensive use of the newer antifungal agents, such as fluconazole, while decreasing the mortality attributed to candidiasis, is resulting in the selection of drug-resistant strains.^{17,18}

ABSTRACT Amphotericin B (AMB) has long been considered the most effective drug in the treatment of serious invasive fungal infections. There are, however, major limitations to its use, due to several adverse effects, including acute infusional reactions and, most relevant, a dose-dependent nephrotoxicity. At least some of these effects are attributed to the aggregation of AMB as a result of its poor water solubility. To overcome this problem, reformulated versions of the drug have been developed, including a micellar dispersion of AMB with sodium deoxycholate (AMBD), its encapsulation into liposomes, or its incorporation into lipidic complexes. The development of nanobiotechnologies provides novel potential drug delivery systems that make use of nanomaterials such as functionalized carbon nanotubes (*f*-CNTs), which are emerging as an innovative and efficient tool for the transport and cellular translocation of therapeutic molecules. In this study, we prepared two conjugates between *f*-CNTs and AMB. The antifungal activity of these conjugates was tested against a collection of reference and clinical fungal strains, in comparison to that of AMB alone or AMBD. Measured minimum inhibition concentration (MIC) values for *f*-CNT–AMB conjugates were either comparable to or better than those displayed by AMB and AMBD. Furthermore, AMBD-resistant *Candida* strains were found to be susceptible to *f*-CNT–AMB 1. Additional studies, aimed at understanding the mechanism of action of the conjugates, suggest a nonlytic mechanism, since the compounds show a major permeabilizing effect on the tested fungal strains only after extended incubation. Interestingly, the *f*-CNT–AMB 1 does not show any significant toxic effect on Jurkat cells at antifungal concentrations.

KEYWORDS: carbon nanotubes · functionalized carbon nanotubes · amphotericin B · antifungal activity · *Candida* spp. · cytotoxicity

As for AMB, in the last 10–15 years, new formulations have been developed that incorporate the drug into small unilamellar liposome carriers (AmBisome) to overcome its toxic effects.^{19,20} We have recently exploited the conjugation of AMB to carbon nanotubes (CNTs), to improve its solubility and decrease its toxic effects, also benefiting the antifungal activity.²¹ Investigations on the potential of CNTs for biomedical applications are rapidly expanding, since functionalized CNTs were found to be biocompatible and nontoxic at the cellular level.^{22–26} In particular, the use of CNTs as carriers for biologically active molecules holds great promises,^{27,28} both as an innovative drug delivery system^{29,30} and for engineering new carriers for genes or siRNAs.^{31,32}

*Address correspondence to a.bianco@ibmc-cnrs.unistra.fr, prato@units.it, rgennaro@units.it.

Received for review September 9, 2010 and accepted December 01, 2010.

Published online December 9, 2010. 10.1021/nn1023522

© 2011 American Chemical Society

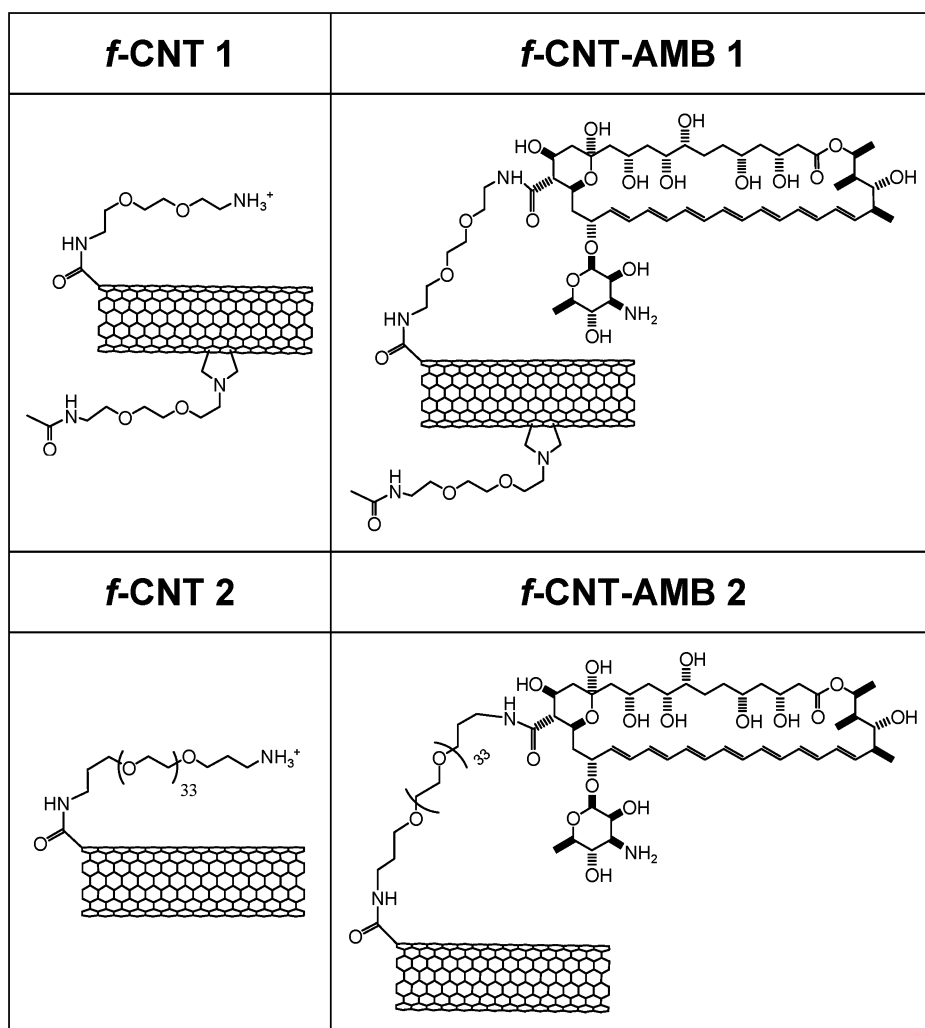


Figure 1. Structure of the CNT conjugates used in this study. The molecular structure of AMB reported in the paper of Wu *et al.* (ref 21) was inadvertently drawn incorrectly. Here we report the correct structure.

In addition, the modulation of molecular functions is another emerging domain in which *f*-CNTs might find potential use.³³ In the field of antimicrobial applications, CNTs have been investigated as supports to induce pathogen aggregation following an appropriate functionalization with sugar-based ligands recognized by receptors on the surface of the microorganisms.^{34–37}

This approach is particularly interesting for the design of new tools for biodefense purposes based on selective interaction of the nanoscale conjugates with targeted pathogens. Alternatively, the conjugation of antimicrobials, such as AMB, to CNTs could lead to several advantages: (i) increased solubility of the molecule, thereby avoiding aggregation, (ii) a more favorable selectivity for target *versus* host cells, leading to an improved therapeutic index, and (iii) improved efficacy, due to a clustering effect and/or to better cellular internalization capacity of the CNTs.

In this study, we have tested the antifungal activity of CNT–AMB-conjugates against a number of fungal reference strains and clinical isolates and compared it to that of AMB alone or AMBD. A relevant outcome of

this screening is the fact that *f*-CNT–AMB 1 is active against *Candida* strains that are highly resistant to AMB and AMBD. In addition, the effect of *f*-CNT–AMB 1 and of AMB on the trans-membrane potential and membrane integrity of selected *C. neoformans* and *C. albicans* strains were compared with the aim of identifying possible differences in the mechanism of action. Finally, we have evaluated the cytotoxicity of the conjugate, used at antifungal concentrations, toward Jurkat cells, a human T-cell leukemia cell line.

RESULTS AND DISCUSSION

Design and Synthesis of *f*-CNT–AMB Conjugates. Following our previous work on the conjugation of AMB to carbon nanotubes,²¹ we expanded the panel of the conjugates and explored the activity of AMB linked to both single- and multiwalled nanotubes (SWNTs and MWNTs, respectively). Similarly to that reported by Wu *et al.*,²¹ we prepared an AMB derivative on multiwalled carbon nanotubes (*f*-CNT–AMB 1) (Figure 1). In addition, we used single-walled carbon nanotubes to prepare a second AMB conjugate (*f*-CNT–AMB 2), in which the dis-

TABLE 1. Antifungal Activity of f-CNT–AMB Conjugates Compared to AMB and AMBD

fungal strain	minimum inhibitory concentration (MIC) ^a (μg/mL)			
	f-CNT–AMB 1	f-CNT–AMB 2	AMB	AMBD ^b
<i>C. neoformans</i> ATCC 90112	2.5 (0.6)	10 (1)	5	1.25
<i>C. neoformans</i> ATCC 52816 ^c	1.25 (0.3)	5 (0.5)	1.25	0.3
<i>C. neoformans</i> ATCC 52817 ^c	0.3 (0.075)	2.5 (0.25)	0.3	0.3
<i>C. neoformans</i> L1	1.25 (0.3)	10 (1)	1.25	0.6
<i>C. albicans</i> ATCC 90029	10 (2.5)	>80 (>8)	>80	>80
<i>C. albicans</i> L21 ^d	10 (2.5)	>80 (>8)	>80	>80
<i>C. parapsilosis</i> ATCC 90118	2.5 (0.6)	10 (1)	5	1.25
<i>C. parapsilosis</i> L51	2.5 (0.6)	20 (2)	5	1.25
<i>C. dubliniensis</i> L70	2.5 (0.6)	20 (2)	1.25	1.25
<i>C. tropicalis</i> L42	1.25 (0.3)	20 (2)	2.5	0.6
<i>C. lusitaniae</i> 1557VC2	2.5 (0.6)	80 (8)	2.5	1.25
<i>C. guilliermondii</i> EMAT 5	2.5 (0.6)	80 (8)	2.5	0.6
<i>C. famata</i> M100 ^{d,e}	2.5 (0.6)	>80 (>8)	10	1.25
<i>C. famata</i> SA550 ^{d,f}	20 (5)	>80 (>8)	>80	>80
<i>R. rubra</i> L8	1.25 (0.3)	80 (8)	2.5	0.6
<i>R. rubra</i> ROMA	2.5 (0.6)	>80 (>8)	10	1.25
<i>P. etchellsii</i> L40	2.5 (0.6)	>80 (>8)	5	1.25
<i>P. etchellsii</i> L41	2.5 (0.6)	>80 (>8)	5	1.25
<i>S. cerevisiae</i> 1557VC1	2.5 (0.6)	10 (1)	5	1.25

^aThe MIC corresponds to the lowest concentration of compound that inhibited visible growth of fungal cells. Results given are mean values of at least two independent determinations performed in duplicate. In this table, the MIC values for f-CNT–AMB 1 and 2 refer to the total weight of conjugate (respective AMB content of 25% and 10% by weight). Data in brackets are the MIC values normalized with respect to AMB content. ^bAMBD: AMB deoxycholate. ^cAcapsular mutants.

^dResistant to amphotericin B. ^eResistant to itraconazole. ^fSusceptible-dose dependent to itraconazole and fluconazole Susceptibility of these selected strains to AMB was also determined using the Etest (AB Biodisk, Solna, Sweden) according to the manufacturer's instructions. Interpretive breakpoints were reported in ref 41.

persibility of CNTs was improved by inserting polyethylene glycol chains. The conjugates **1** and **2** contained, respectively, 25% and 10% of AMB by weight. f-CNTs devoid of AMB were used as a control.

Antifungal Activity of the f-CNT–AMB Conjugates. The antifungal activity of the two f-CNT–AMB conjugates and of their respective controls (structures shown in Figure 1) was first evaluated against 10 strains of *Candida* spp. (8 clinical isolates and 2 ATCC reference strains) and 4 strains of *C. neoformans* (1 clinical isolate and 3 ATCC reference strains). The activity was compared to that of AMB alone and of AMBD, the colloidal dispersion formulation in clinical use (Table 1). Antifungal susceptibility testing was then extended to other fungal species by including *Pichia*, *Rhodotorula*, and *Saccharomyces* strains. Several of the tested strains were resistant to commonly used antifungal drugs including AMB, itraconazole, and fluconazole, as indicated in Table 1.

The f-CNT–AMB **1** and **2** conjugates were both found to display a broad-spectrum antifungal activity, although with a variable potency against the strains tested. f-CNT–AMB **1** globally displayed the most potent and broad-spectrum activity, with MIC values lower than 10 μg/mL against most of the microorganisms tested. The only exception was the *C. famata* SA550

strain, which showed a MIC value of 20 μg/mL. The second conjugate (f-CNT–AMB **2**) exhibited a reasonably good antifungal activity with MIC values ranging from 5 to 20 μg/mL for most of the tested strains. Interestingly, the two acapsular strains of *C. neoformans* are from 2 to 8 fold more susceptible to the conjugates than the parental capsulated strain, indicating that the polysaccharidic capsule likely constitutes an effective barrier for the drug. A similarly increased susceptibility of the acapsular strain versus the capsulated strain is also shown by AMB and AMBD (Table 1). No antifungal activity (MIC >80 μg/mL) was shown by the functionalized CNTs (f-CNT **1** and **2**) devoid of AMB, which were used as a control (data not shown). The activity of the conjugates is thus not ascribable to a direct action of the f-CNTs. In addition, the antifungal activity shown by f-CNT–AMB **1** against some drug-resistant strains suggests that the conjugation of AMB to MWNTs favors in some way the activity of this antifungal drug. The majority of the AMB-resistant strains characterized so far have quantitative or qualitative alterations in the sterol composition of their cell membranes;³⁸ it is thus likely that the AMB conjugated to the nanotubes favors interaction with residual membrane sterols, in addition to having an improved solubility.

Taking into account that the AMB content by weight in the two conjugates is 25% and 10% for f-CNT–AMB **1** and **2**, respectively, it is clearly evident that the conjugates are in general significantly more active than AMB and somewhat more active than AMBD (Table 1). In particular, f-CNT–AMB **2** displays MIC values that are frequently better than those of AMB alone and comparable to those of AMBD, with the notable exception of *C. lusitaniae*, *C. guilliermondii*, *C. famata*, *Rhodotorula*, and *Pichia* strains (Table 1). The lower activity of f-CNT–AMB **2** against these strains has no explanation at present, although it may depend on a lower drug density on the surface of the f-CNTs. The highest activity is displayed by f-CNT–AMB **1**, which shows MIC values that are generally better than those of AMBD. Of note is the potent activity of this conjugate against strains resistant to both AMB and AMBD, such as *C. albicans* ATCC 90029 and L21, and *C. famata* SA550 (Table 1).

Killing Kinetics of Fungal Strains by f-CNT–AMB Conjugates.

The antifungal activity of f-CNT–AMB **1** and **2** was further investigated by analyzing their killing kinetics against two representative clinical isolates: *C. neoformans* L1 and *C. albicans* L21. The latter strain was not tested with the f-CNT–AMB **2** and with AMBD as it was resistant to these compounds (MIC >80 μg/mL). The f-CNT–AMB **2** did not cause any decrease in the number of viable *C. neoformans* cells when added at its MIC value, and caused a reduction of over 90% only at a concentration 4 times the MIC at 4 h incubation (Figure 2A). The f-CNT–AMB **1** conjugate did not cause any cell viability reduction at 2 times its MIC value (2.5 μg/

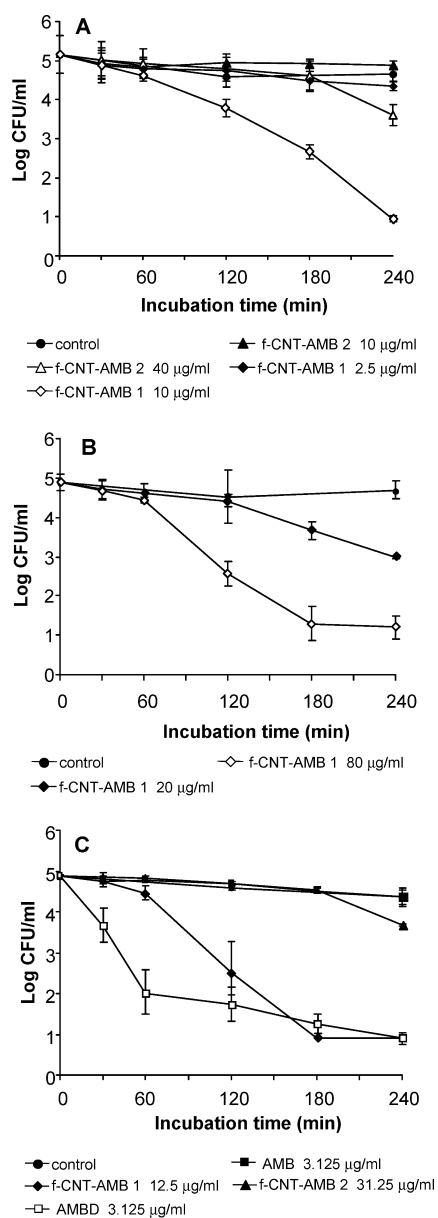


Figure 2. Killing kinetics of *f*-CNT-AMB 1 and 2 against *C. neoformans* L1 (A and C) and *C. albicans* L21 (B). In panel C, the *f*-CNT-AMB conjugates were added at an amount that allowed reaching a final concentration of conjugated AMB of 3 µg/mL, equal to that of AMB or AMBD alone. Fungal cells were incubated in RPMI-1640 medium, and at the indicated times survivors were serially diluted in PBS and plated to allow colony counts. Results are mean values \pm standard deviation (SD) of at least four independent determinations.

mL), while over 99.99% of the cells were killed at 8 times the MIC at 4 h incubation (Figure 2A). The killing of *C. albicans* by *f*-CNT-AMB 1 required a concentration higher than that necessary to inactivate *C. neoformans* (Figure 2B). However, a reduction in viable cells of 90% and 99.9% was respectively obtained at concentrations of 2 times (20 µg/mL) and 8 times (80 µg/mL) the MIC value, after 3 h incubation. The time required for the fungicidal activity of AMB is species- and concentration-dependent. However, in all cases, to observe a significant fungicidal activity it was necessary to use a drug

concentration higher than that corresponding to the MIC value, as already reported for AMBD.³⁹ Despite the differences in the killing kinetics displayed by the CNT conjugates tested, it is interesting to note that *f*-CNT-AMB 1 inactivates *C. neoformans* cells more rapidly and effectively than AMB and *f*-CNT-AMB 2, when the compounds are compared at the same amount of drug (Figure 2C). Under these conditions, AMBD showed more rapid killing kinetics than *f*-CNT-AMB 1, even though, from 3 h on, the final killing capacity was comparable (Figure 2C). Finally, it is worth noting that the CNT conjugates are dissolved in water, while for AMB the presence of an organic solvent is necessary, as reported in previous studies.^{39,40}

Effects of the *f*-CNT-AMB Conjugates on Fungal Membrane Potential. In an attempt to understand the mechanism by which the *f*-CNT-AMB conjugates inactivate *C. neoformans* and *C. albicans* cells, the effect of the most active compound *f*-CNT-AMB 1 on the transmembrane potential of these fungi was evaluated by flow cytometry. Cell membrane depolarization was assessed by the addition of bis-(1,3-dibutylbarbituric acid)trimethine oxonol [DiBAC₄(3)]. This probe preferentially enters and fluorescently labels the cells whose membrane potential has collapsed. In the absence of treatment (Figure 3), the large majority of the cells was undamaged (filled bar charts) and showed mean fluorescence intensities (MFI) of 6.4 ± 1.1 and 12.4 ± 4.6 , respectively, for *C. neoformans* and *C. albicans*. This indicates that most of the fungal cells maintained a normal transmembrane potential, with only a low percentage showing a depolarized membrane (empty bar charts; $9.7 \pm 3.3\%$ and $16.6 \pm 2\%$ for *C. neoformans* and *C. albicans*, respectively). After 2–4 h incubation with 10 µg/mL of *f*-CNT 1 and *f*-CNT-AMB 1, the percentage of depolarized *C. neoformans* cells did not increase significantly with respect to the untreated control (data not shown). Overnight treatment (16 h) of the cells with the unconjugated control *f*-CNT 1 induced only a slight increase in the percentage of depolarized cells with respect to untreated cells ($13.3 \pm 6.9\%$ and $21.7 \pm 3.9\%$ for *C. neoformans* and *C. albicans*, respectively), which is not statistically significant (Figure 3). In contrast, the percentage of depolarized, highly fluorescent cells (MFI = 139.4 ± 43.8) remarkably increased to $92.7 \pm 0.4\%$ (Figure 3A) after incubation with 10 µg/mL of *f*-CNT-AMB 1. These results indicate that the functionalized nanotubes alone do not cause a significant depolarization of the fungal cells, while conjugation with AMB induces an almost complete depolarization of *C. neoformans* cells, although with a slow kinetics, which may indicate this as a secondary effect. Overnight exposure to unconjugated AMB induced depolarization of the fungal cells (MFI = 81.3 ± 10.3), but only half of the population (approximately 47%) was strongly depolarized (MFI = 298.3 ± 65.2), while the remaining cells were less affected (Figure 3A). The reason for the bimodal depolar-

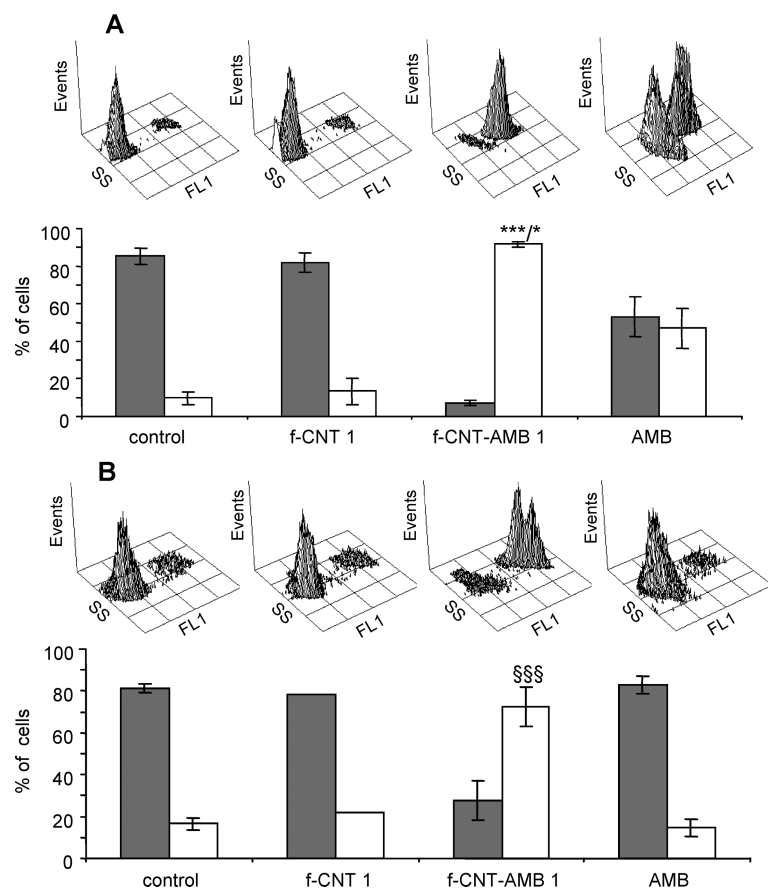


Figure 3. Dual-parameter dot plot of the side scatter intensity (SS) versus DiBAC₄(3) fluorescence intensity (FL1) and bar charts of the percentage of undamaged or depolarized cells after 16 h incubation of *C. neoformans* L1 (panel A) and *C. albicans* L21 (panel B) with *f*-CNT 1, *f*-CNT-AMB 1, and AMB alone. *f*-CNT-AMB 1, *f*-CNT 1, and AMB were used at 10 μ g/mL. Filled and empty bar charts respectively represent undamaged and depolarized cells. Results are mean values \pm SD of at least four independent determinations. The scale of the SS and FL1 axes in the dot plots is logarithmic: (***) $p < 0.001$ vs control and *f*-CNT 1 groups, (*) $p < 0.05$ vs AMB group; (SSS) $p < 0.001$ vs control, *f*-CNT 1, and AMB groups (Student–Newman–Keuls Multiple Comparisons Test, ANOVA).

ization pattern of AMB-treated cells is yet unknown, although it could be ascribed to the presence of a mixture of water-soluble monomers of AMB and of oligomers that form insoluble aggregates.²⁰ Similarly to *C. neoformans*, the fluorescence intensity of *C. albicans* after 16 h incubation with *f*-CNT-AMB 1 (Figure 3B) was strongly shifted with respect to untreated cells (MFI = 229.9 ± 52.4 vs 12.4 ± 4.6 for untreated cells), revealing again a remarkable depolarization of the cellular population ($72.4 \pm 9\%$ of highly fluorescent cells). In contrast, treatment with AMB alone did not cause a statistically significant depolarization (MFI = 12.6 ± 5.4), in agreement with the AMB-resistant phenotype of this strain. Although the interaction of AMB with the sterols present at the plasma membrane level is considered the first step of its mechanism of action,³⁸ a depolarizing effect is detectable only after overnight treatment, indicating that the initial alterations of membrane permeability caused by AMB do not induce a notable variation of its membrane potential.

Effect of the *f*-CNT-AMB Conjugates on the Membrane

Integrity. The slow depolarizing effect revealed by the DiBAC₄(3) probe suggests that the *f*-CNT-AMB conju-

gates do not rapidly permeabilize the fungal membranes. To evaluate the kinetics of a putative membrane damage caused by the conjugates, untreated and treated cells were incubated with propidium iodide (PI), a well-known fluorescent probe used to evaluate membrane integrity. Treatment of *C. neoformans* for 4 h with 10 μ g/mL of *f*-CNT-AMB 1 did not induce any significant membrane permeabilization with only 7% of PI-positive cells, a value comparable to the control (data not shown). Lengthening the incubation time up to 16 h increased PI-positive cells to 40%. A comparable result was obtained after treatment of *C. neoformans* with 10 μ g/mL of AMB for 16 h (Figure 4A). A remarkably higher permeabilizing effect was observed after treatment of *C. albicans* with 10 μ g/mL of *f*-CNT-AMB 1 for 16 h, with 80% of PI-positive cells vs 7% and 5% for, respectively, the untreated control and unconjugated *f*-CNT. In contrast, after incubation with AMB, the percentage of PI positive cells was not statistically different from that of untreated or *f*-CNT 1-treated cells (Figure 4B). This is an expected result, as the strain tested is AMB-resistant, as indicated by its MIC value (see Table 1). Altogether, these results sug-

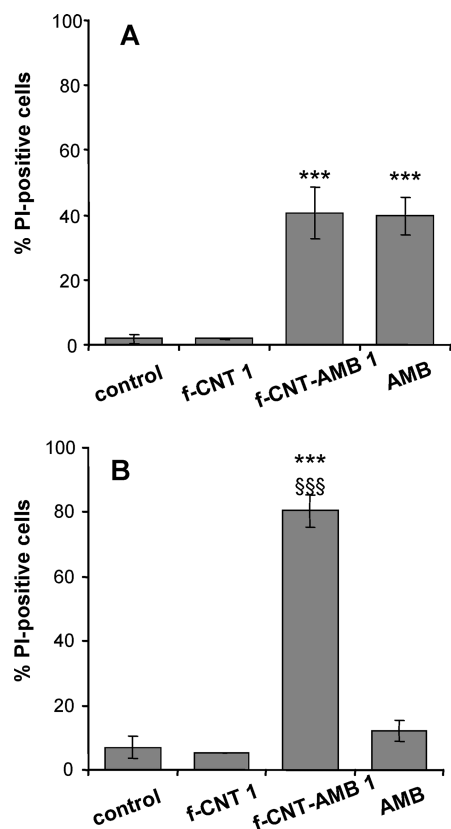


Figure 4. Percentage of PI-positive (permeabilized) cells after incubation of *C. neoformans* L1 (panel A) and *C. albicans* L21 (panel B) for 16 h with 10 $\mu\text{g/mL}$ of *f*-CNT 1, *f*-CNT-AMB 1, or AMB alone. Results are mean values \pm SD of at least four independent determinations. (***) $p < 0.001$ vs control and *f*-CNT 1 groups; (§§§) $p < 0.001$ vs control and AMB groups (Student–Newman–Keuls Multiple Comparisons Test, ANOVA).

gest that the *f*-CNT-AMB conjugates do not affect yeast cells by damaging their membranes due to the presence of the CNT, as indicated by the fact that unconjugated *f*-CNTs are inactive. Moreover, compounds that act *via* membrane permeabilization, such as some lytic antimicrobial peptides,⁴¹ have kinetics of PI-uptake much faster than that here reported. The longer time exposure necessary for observing evident depolarizing and permeabilizing effects (Figures 3 and 4) compared to the incubation time required for the fungicidal activity (see Figure 2), suggests that the effects of *f*-CNT-AMB on the fungal plasma membranes are a consequence rather than a cause of cell death.

It is known that interaction of AMB with sterols, in particular with ergosterol present in the fungal plasma membrane, induces the formation of transmembrane pores or channels that are made of eight drug molecules linked to form a barrel stave-like structure with an internal hydrophilic channel of approximately 8 Å diameter.³⁸ The AMB pores alter the membrane permeability, causing leakage of K^+ and of other vital cytoplasmic components and entry of hydrogen ions. These effects may lead to membrane disruption and possible fungal cell death.³⁸ This is the most widely accepted

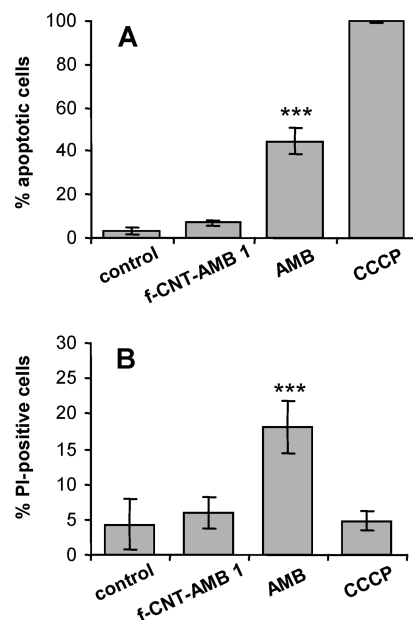


Figure 5. Percentage of apoptotic (A) and/or necrotic (B) Jurkat cells after treatment with 10 $\mu\text{g/mL}$ of *f*-CNT-AMB 1 or AMB. After incubation for 16 h at 37 °C, the cells were stained with DiOC₆ (A) and PI (B) and analyzed by flow cytometry. CCCP was used as a positive control for collapse of mitochondrial transmembrane potential. Results are mean values \pm SD of at least four independent determinations. (***) $p < 0.001$ vs control, *f*-CNT-AMB 1, and CCCP treatment groups (Student–Newman–Keuls Multiple Comparisons Test, ANOVA).

model for the mechanism of action of AMB, although not the only one. In fact, several studies have shown that killing of fungal cells can be a consequence of AMB-induced oxidative stress. It is thus possible that the effect of *f*-CNT-AMB 1 on fungal cells is not mediated by pore formation but by a different mechanism such as, for instance, oxidative damage.⁴² Further studies are necessary to clarify this hypothesis.

Cytotoxic Effects of *f*-CNT-AMB Conjugates on the Jurkat Human Cell Line. Considering the improved activity of AMB against fungal cells as a result of its conjugation to CNTs, we investigated whether this was paralleled by an increased toxicity toward mammalian cells. The Jurkat cell line, derived from a human T-cell leukemia, was used as a model for circulating cells. The cells were incubated up to 16 h with *f*-CNT-AMB 1 or with AMB, both at a concentration of 10 $\mu\text{g/mL}$, and then analyzed by flow cytometry following double staining with PI and 3,3'-dihexyloxy carbocyanide iodide (DiOC₆). The former fluorescent probe detects plasma membrane damage, while the latter is a cationic, lipophilic dye that selectively stains mitochondria and whose fluorescence emission decreases when the mitochondrial inner membrane potential collapses. PI is used to discriminate necrotic and late apoptotic cells, which have lost plasma membrane integrity and then its barrier properties, from early apoptotic cells that still have an intact membrane but show a decreased DiOC₆ fluorescence. The results reported in Figure 5 show that AMB

alone at 10 $\mu\text{g}/\text{mL}$ induces apoptosis in over 40% of the Jurkat cell population, with approximately 20% of the cells that are necrotic/late apoptotic. Treatment of cells with the same amount of AMB conjugated to CNTs (compound *f*-CNT-AMB **1**) results in $7.2 \pm 1.2\%$ of apoptotic cells and $6.0 \pm 2.3\%$ of necrotic cells, a level comparable and not statistically different from that of control cells ($3.2 \pm 1.4\%$ and $4.3 \pm 3.65\%$ of apoptotic and necrotic cells, respectively). Figure 5 also shows the effect of carbonyl cyanide 3-chlorophenylhydrazone (CCCP), a selective mitochondrial depolarizing agent used as positive control, which induces depolarization in $99.6 \pm 0.28\%$ of the cell population, while leaving the percentage of necrotic cells at a level (4.74 ± 1.37) not significantly different from that of the control. It is important to note that *f*-CNT-AMB **1** does not show any significant toxic effect *in vitro* on Jurkat mammalian cells at antifungal concentrations. This has been already observed by using AMB conjugated to carbon nanotubes at a concentration up to 10 μg mass of drug linked to the nanotubes.²¹

It has been reported that the various aggregation forms of AMB interact with the sterols present in the membranes in different ways. In fact, AMB induces leakage of K^+ through the mammalian cholesterol-containing membranes only beyond a certain concentration threshold, which corresponds to the formation of self-associated AMB (oligomers). Conversely, the toxicity for the ergosterol-containing membranes, a characteristic feature of fungal cells, is due to the monomeric form of AMB.²⁰ The conjugation of the drug with CNTs might thus prevent its aggregation and then decrease its toxicity toward mammalian cells, while maintaining it in a monomeric form that favors the antifungal activity.

CONCLUSIONS

Functionalized carbon nanotubes are emerging as a new material for biomedical applications.⁴³ In this context, we previously demonstrated the potential of *f*-CNT technology in the field of antimicrobial therapy²¹ by showing that conjugation of AMB to *f*-CNTs decreased the cytotoxic effects of the drug against mammalian cells, while preserving its high antifungal activity. In the present work, we have expanded those investigations by exploring new CNT-AMB conjugates and by testing their activity against numerous fungal species, including drug-resistant strains. Both single- and multiwalled carbon nanotubes were modified with AMB. The conjugates displayed good water solubility. In particular,

f-CNT-AMB **1**, which is based on MWNTs, was more soluble than *f*-CNT-AMB **2**, for which SWNTs were used. This is not surprising, as it is known that SWNTs are more difficult to disperse and maintain them individualized under physiological conditions.⁴⁴ In addition, the type and degree of functionalization of the two conjugates here investigated certainly play a key role in determining the solubility properties. This behavior has also an impact on the antifungal activity. Indeed, the multiwalled compound *f*-CNT-AMB **1** is overall more active than the SWNT conjugate, also when compared by AMB content.

Interestingly, we found that *f*-CNT-AMB **1** also exerts a significant activity against strains that are AMB-resistant, as indicated by the efficacy of this compound against *C. albicans* L21 and ATCC 90029, and *C. famata* M100 and SA550 (Table 1), making this conjugate a very promising hit for future development. The reason why this compound is active against drug-resistant strains, at variance with AMB, AMBD, and *f*-CNT-AMB **2**, is not known. A hypothesis that could explain this behavior is the multivalence effect that is obtained when a high number of molecules of an active species, in this case AMB, is conjugated to the surface of single nanostructures such as functionalized CNTs. In the case of *f*-CNT-AMB **1**, in which the total drug load is 25% by weight, this could lead to an improved binding affinity to the drug target on the fungal surface, thereby overcoming the resistant phenotype that is frequently due to quantitative or qualitative alterations in the sterol composition of the membrane,^{38,45,46} such as to a decreased presence of ergosterol, substituted by precursor compounds that show a lower affinity for AMB.⁴⁷

In the literature, there are several formulations based on nanoparticles that modulate the activity of AMB.⁴⁸ Chemical conjugation was exploited mainly on polymeric materials rather than on organic or inorganic nanoparticles or on different nano-objects. We believe that our approach, based on CNTs, represents a promising alternative to improve the pharmacological profile of AMB and can be extended to other antimicrobial agents for the treatment of infectious diseases.

In addition, the conjugates here reported display a much reduced toxicity *in vitro* against mammalian cells with respect to AMB, adding further value to our approach. This observation is in line with others showing that properly functionalized CNTs have no obvious toxicity *in vitro* and *in vivo* in animal models,^{21,44,49–52} in contrast to nonfunctionalized nanotubes that are toxic to cells and animals.^{53–56}

METHODS

Chemicals and Carbon Nanotubes. All reagents were obtained from commercial suppliers and used without further purification. SWNTs were purchased from Carbon Nanotechnology Inc. (Houston, USA) and were CNI grade (Lot No. R0496). Purified

MWNTs were purchased from Nanostructured & Amorphous Materials Inc. (Houston, USA) and were 95% pure (stock no. 1240XH). Their outer average diameter was between 20 and 30 nm and their length was between 0.5 and 2 μm . AMB and AMBD (a colloidal dispersion of AMB and sodium deoxycholate) were

purchased from Sigma-Aldrich. AMB was freshly dissolved in 10% (v/v) of DMSO and AMBD was dissolved in Milli-Q water. The final concentration of DMSO in the antifungal assays never exceeded 0.2% (v/v).

Preparation of *f*-CNT–AMB Conjugates. The MWNTs and the SWNTs were functionalized by slightly modifying a previously described procedure^{21,44} to obtain *f*-CNT **1** and *f*-CNT **2**, respectively (Figure 1) (see Supporting Information for experimental details). These two precursors were then reacted as reported by Wu *et al.*²¹ with a solution of Fmoc–AMB–OH to obtain the respective conjugates *f*-CNT–AMB **1** and *f*-CNT–AMB **2** (Figure 1). The two derivatives differ by the type of nanotube support (MWNTs and SWNTs, respectively, for *f*-CNT **1** and *f*-CNT **2**), the length of the PEG chain linking AMB to the CNTs, and the degree of substitution with the drug. The conjugate **1** has a TEG linker and an AMB content of 25% by weight. The conjugate **2** contains a PEG linker, with a repeat of 33 monomers of oxyethylene, and an AMB content of 10% by weight. In addition, *f*-CNT–AMB **1** contains acetylated TEG groups to increase water solubility (2% by weight). Both CNT conjugates were dissolved in Milli-Q water and stored at –20 °C. The compounds were characterized by transmission electron microscopy (TEM) performed on a Hitachi H600 microscope, working at different accelerating voltage and magnification.

Fungal Strains and Growth Conditions. Several different clinical isolates and ATCC reference fungal strains were used in this study. The former included *Candida* spp., *Cryptococcus neoformans*, *Rhodotorula rubra*, *Saccharomyces cerevisiae*, and *Pichia etchellsii*, and were mostly collected from immuno-compromised patients. The latter comprised the capsulated ATCC 90112 strain of *Cryptococcus neoformans* as well as the acapsular mutants ATCC 52816 and ATCC 52817, *Candida albicans* ATCC 90029, and *Candida parapsilosis* ATCC 90018. Fungi were grown on Sabouraud agar plates at 30 °C for 48 h. Inocula were prepared by picking and suspending five colonies in 5 mL of sterile buffered saline solution containing 10 mM sodium phosphate and 145 mM NaCl, pH 7.4 (phosphate-buffered saline, PBS). The turbidity of the fungal suspensions was measured at 600 nm and was adjusted to obtain the appropriate inoculum according to previously derived curves relating the number of colony forming units (CFUs) with absorbance.

Antifungal Activity. The antifungal activity of *f*-CNT–AMB conjugates, their controls devoid of AMB, AMB alone, and AMBD (see Table 1) was evaluated by the broth microdilution susceptibility test performed according to the guidelines of the Clinical and Laboratory Standards Institute (CLSI), formerly National Committee for Clinical Laboratory Standards, to determine the minimum inhibitory concentration (MIC) values. 2-Fold serial dilutions of each compound were prepared in 96-well polypropylene microtiter plates (Sarstedt, Germany) in RPMI-1640 medium (Sigma-Aldrich) to a final volume of 50 μ L. Each series included a well without addition of any compound, as a growth control. A total of 50 μ L of the adjusted inoculum, diluted in RPMI-1640 medium, was then added to each well to obtain a final concentration of approximately 5×10^4 CFUs/mL. Samples were incubated at 30 °C for 48 h. The MIC value was taken as the lowest concentration of antifungal agent resulting in the complete inhibition of visible fungal growth after 48 h incubation. Data are the mean of up to six independent determinations performed in duplicate with values differing by one dilution at the most.

Killing Kinetics Assays. Killing kinetics were determined using cultures of *C. albicans* L21 and *C. neoformans* L1 diluted in fresh RPMI-1640 medium to give approximately 5×10^4 CFUs/mL. *f*-CNT–AMB conjugates were added at different concentrations and the suspensions were then incubated in a shaking water bath at 30 °C. At the indicated times, an aliquot of each sample was removed, serially diluted with PBS, and plated in duplicate on Sabouraud agar. The number of colonies was counted after incubation of the plates for 48 h at 30 °C. Data are the mean of at least four independent determinations with comparable results.

Evaluation of Alteration of the Fungal Membrane by Flow Cytometric Assays. Specific flow cytometric assays were used to evaluate the transmembrane potential and the membrane permeabilization of fungal cells treated with the *f*-CNT–AMB conjugates. For these analyses, *C. albicans* L21 and *C. neoformans* L1, subcul-

tured on Sabouraud agar, were diluted in RPMI-1640 medium to 1×10^5 CFUs/mL. Aliquots of the fungal suspension were then incubated with or without the *f*-CNT-conjugates for 2–16 h at 30 °C. At the end of the incubation time, the fungal suspensions were incubated in the dark for 60 min at 30 °C with DiBAC₄(3) (Invitrogen Co., Carlsbad, CA) at a final concentration of 1 μ M, to evaluate modifications of the transmembrane potential. To monitor alterations in membrane integrity following treatment with the CNT-derivatives, a filtered solution of PI (Sigma-Aldrich), at a final concentration of 10 μ g/mL, was incubated for 60 min at 30 °C with each sample. An untreated sample of fungal cells, pelleted and resuspended in cold absolute ethanol for 30 min at –20 °C was used as a positive control of permeabilization. After centrifugation at 1000g for 10 min, the ethanol was removed by aspiration, the pellet was suspended in RPMI-1640 medium, and the PI was added as reported above. The fluorescence intensity was detected with a Cytomics FC 500 instrument (Beckman-Coulter, Inc., Fullerton, CA) equipped with an argon laser (488 nm, 5 mW) and using a photomultiplier tube fluorescence detector for green (525 nm) or red (610 nm) filtered light. The detectors were set on logarithmic amplification. Optical and electronic noise were eliminated by setting an electronic gating threshold on the forward scattering detector, while the flow rate was kept at a data rate below 200 events/second to avoid cell coincidence. For each sample, at least 10000 events were acquired and stored as list mode files.

All the experiments with the fluorescent probes were conducted in triplicate and the data analyses were performed with the WinMDI software (Dr J. Trotter, Scripps Research Institute, La Jolla, CA, USA). Data are expressed as mean \pm SD.

Cell Culture and Cytotoxicity Assay. The Jurkat human T-lymphoma cell line was cultured in RPMI-1640 (Cambrex Bioscience) supplemented with gentamicin (10 μ g/mL) and 10% of heat-inactivated fetal bovine serum. Cells were grown in suspension at 37 °C in a humidified atmosphere in the presence of 5% CO₂. For the tests, cell suspensions were prepared at a final density of 5×10^5 cells/mL in 2 mL of medium containing *f*-CNT–AMB **1** or AMB at a final concentration of 10 μ g/mL. After addition of AMB, the final percentage of DMSO in the cell cultures was always lower than 0.1% (v/v). The cells were then incubated at 37 °C up to 16 h. To evaluate apoptosis induction, at the end of the incubation time, the cells were stained in the dark at 37 °C for 15 min with 50 nM of DiOC₆ (FluoProbes, Interchim, Montlucon Cedex, France), a fluorescent probe used to measure the mitochondrial transmembrane potential in intact cells. A positive control for collapse of mitochondrial transmembrane potential was obtained by incubating a cell suspension at 37 °C with 50 μ M of the uncoupler CCCP for 15 min. After treatment with DiOC₆, to test cell viability, the samples were washed twice with 2 mL of PBS and then stained in the dark at room temperature with 10 μ g/mL PI for 10 min. Cells were analyzed by flow cytometry as described above, acquiring at least 10000 events for each sample and storing the results as list mode files.

Statistical Analysis. Data are expressed as mean \pm SD. Significance of differences among groups was assessed by using the program Instat (GraphPad Software Inc., San Diego, CA) and performed by an analysis of variance between groups (ANOVA) followed by the Student–Newman–Keuls post test. Values of $p < 0.05$ were considered statistically significant.

Acknowledgment. This work was supported by the CNRS, the University of Trieste, INSTM, MIUR (Cofin Prot. 20085M275S and Fibr RBIN04HC3S) and Regione Friuli Venezia-Giulia. W.W. is grateful to French Ministry for Research and New Technologies for a postdoctoral fellowship. TEM images were recorded at the RIO Microscopy Facility Platform of Esplanade (Strasbourg, France). We wish to thank Cécilia Ménard-Moyon for her help with TEM.

Supporting Information Available: Detailed experimental procedure for the preparation of *f*-CNT–AMB conjugates. This material is available free of charge via the Internet at <http://pubs.acs.org>.

REFERENCES AND NOTES

- Petrikos, G.; Skiada, A. Recent Advances in Antifungal Chemotherapy. *Int. J. Antimicrob. Agents*. **2007**, *30*, 108–117.
- Burke, D.; Lal, R.; Finkel, K. W.; Samuels, J.; Foringer, J. R. Acute Amphotericin B Overdose. *Ann. Pharmacother.* **2006**, *40*, 2254–2259.
- Slavin, M. A.; Szer, J.; Grigg, A. P.; Roberts, A. W.; Seymour, J. F.; Sasadeusz, J.; Thursky, K.; Chen, S. C.; Morrissey, C. O.; Heath, C. H.; *et al.* Guidelines for the Use of Antifungal Agents in the Treatment of Invasive Candida and Mould Infections. *Intern. Med. J.* **2004**, *34*, 192–200.
- Charvalos, E.; Tzatzarakis, M. N.; Van Bambeke, F.; Tulkens, P. M.; Tsatsakis, A. M.; Tzanakakis, G. N.; Mingeot-Leclercq, M. P. Water-Soluble Amphotericin B–Polyvinylpyrrolidone Complexes with Maintained Antifungal Activity against *Candida* spp. and *Aspergillus* spp. and Reduced Haemolytic and Cytotoxic Effects. *J. Antimicrob. Chemother.* **2006**, *57*, 236–244.
- Falagas, M. E.; Ntziora, F.; Betsi, G. I.; Samonis, G. Caspofungin for the Treatment of Fungal Infections: A Systematic Review of Randomized Controlled Trials. *Int. J. Antimicrob. Agents*. **2007**, *29*, 136–143.
- Jain, L. R.; Denning, D. W. The Efficacy and Tolerability of Voriconazole in the Treatment of Chronic Cavitory Pulmonary Aspergillosis. *J. Infect.* **2006**, *52*, 133–137.
- Kirkpatrick, W. R.; Coco, B. J.; Patterson, T. F. Sequential or Combination Antifungal Therapy with Voriconazole and Liposomal Amphotericin B in a Guinea Pig Model of Invasive Aspergillosis. *Antimicrob. Agents Chemother.* **2006**, *50*, 1567–1569.
- Klein, K. C.; Blackwood, R. A. Topical Voriconazole Solution for Cutaneous Aspergillosis in a Pediatric Patient after Bone Marrow Transplant. *Pediatrics* **2006**, *118*, 506–508.
- Sambatakou, H.; Dupont, B.; Lode, H.; Denning, D. W. Voriconazole Treatment for Subacute Invasive and Chronic Pulmonary Aspergillosis. *Am. J. Med.* **2006**, *119*, 517–524.
- Singh, N.; Limaye, A. P.; Forrest, G.; Safdar, N.; Munoz, P.; Pursell, K.; Houston, S.; Rosso, F.; Montoya, J. G.; Patton, P.; *et al.* Combination of Voriconazole and Caspofungin as Primary Therapy for Invasive Aspergillosis in Solid Organ Transplant Recipients: A Prospective, Multicenter, Observational Study. *Transplantation* **2006**, *81*, 320–326.
- Barchiesi, F.; Spreghini, E.; Santinelli, A.; Fothergill, A. W.; Pisa, E.; Giannini, D.; Rinaldi, M. G.; Scalise, G. Posaconazole Prophylaxis in Experimental Systemic Zygomycosis. *Antimicrob. Agents Chemother.* **2007**, *51*, 73–77.
- Greenberg, R. N.; Mullane, K.; van Burik, J. A.; Raad, I.; Abzug, M. J.; Anstead, G.; Herbrecht, R.; Langston, A.; Marr, K. A.; Schiller, G.; *et al.* Posaconazole as Salvage Therapy for Zygomycosis. *Antimicrob. Agents Chemother.* **2006**, *50*, 126–133.
- van Burik, J. A.; Hare, R. S.; Solomon, H. F.; Corrado, M. L.; Kontoyiannis, D. P. Posaconazole Is Effective as Salvage Therapy in Zygomycosis: A Retrospective Summary of 91 Cases. *Clin. Infect. Dis.* **2006**, *42*, 61–65.
- Gupta, S.; Almyroudis, N. G.; Battiwalla, M.; Bambach, B. J.; McCarthy, P. L.; Proefrock, A. D.; Ball, D.; Papham, P.; Varma, A.; Kwon-Chung, J.; *et al.* Successful Treatment of Disseminated Fusariosis with Posaconazole during Neutropenia and Subsequent Allogeneic Hematopoietic Stem Cell Transplantation. *Transplant Infect. Dis.* **2007**, *9*, 156–160.
- Raad, I. I.; Hachem, R. Y.; Herbrecht, R.; Graybill, J. R.; Hare, R.; Corcoran, G.; Kontoyiannis, D. P. Posaconazole as Salvage Treatment for Invasive Fusariosis in Patients with Underlying Hematologic Malignancy and Other Conditions. *Clin. Infect. Dis.* **2006**, *42*, 1398–1403.
- Negróni, R.; Tobon, A.; Bustamante, B.; Shikanai-Yasuda, M. A.; Patino, H.; Restrepo, A. Posaconazole Treatment of Refractory Eumycetoma and Chromoblastomycosis. *Rev. Inst. Med. Trop. Sao Paulo.* **2005**, *47*, 339–346.
- Andes, D.; Forrest, A.; Lepak, A.; Nett, J.; Marchillo, K.; Lincoln, L. Impact of Antimicrobial Dosing Regimen on Evolution of Drug Resistance *In Vivo*: Fluconazole and *Candida albicans*. *Antimicrob. Agents Chemother.* **2006**, *50*, 2374–2383.
- Andes, D.; Lepak, A.; Nett, J.; Lincoln, L.; Marchillo, K. *In Vivo* Fluconazole Pharmacodynamics and Resistance Development in a Previously Susceptible *Candida albicans* Population Examined by Microbiologic and Transcriptional Profiling. *Antimicrob. Agents Chemother.* **2006**, *50*, 2384–2394.
- Adler-Moore, J.; Proffitt, R. T. AmBisome: Liposomal Formulation, Structure, Mechanism of Action and Pre-Clinical Experience. *J. Antimicrob. Chemother.* **2002**, *49*, 21–30.
- Torrado, J. J.; Espada, R.; Ballesteros, M. P.; Torrado-Santiago, S. Amphotericin B Formulations and Drug Targeting. *J. Pharm. Sci.* **2008**, *97*, 2405–2425.
- Wu, W.; Wieckowski, S.; Pastorin, G.; Benincasa, M.; Klumpp, C.; Briand, J. P.; Gennaro, R.; Prato, M.; Bianco, A. Targeted Delivery of Amphotericin B to Cells by Using Functionalized Carbon Nanotubes. *Angew. Chem., Int. Ed.* **2005**, *44*, 6358–6362.
- Lacerda, L.; Bianco, A.; Prato, M.; Kostarelos, K. Carbon Nanotubes as Nanomedicines: From Toxicology to Pharmacology. *Adv. Drug Delivery Rev.* **2006**, *58*, 1460–1470.
- Bianco, A.; Kostarelos, K.; Prato, M. Applications of Carbon Nanotubes in Drug Delivery. *Curr. Opin. Chem. Biol.* **2005**, *9*, 674–679.
- Bianco, A.; Kostarelos, K.; Partidos, C. D.; Prato, M. Biomedical Applications of Functionalised Carbon Nanotubes. *Chem. Commun. (Cambridge)*. **2005**, 571–577.
- Lin, Y.; Taylor, S.; Li, H.; Fernando, K. A. S.; Qu, L.; Wang, W.; Gu, L.; Zhou, B.; Sun, Y.-P. Advances toward Bioapplications of Carbon Nanotubes. *J. Mater. Chem.* **2004**, *14*, 527–541.
- Kam, N. W.; Liu, Z.; Dai, H. Carbon Nanotubes as Intracellular Transporters for Proteins and DNA: An Investigation of the Uptake Mechanism and Pathway. *Angew. Chem., Int. Ed.* **2006**, *45*, 577–581.
- Kostarelos, K.; Bianco, A.; Prato, M. Promises, Facts and Challenges for Carbon Nanotubes in Imaging and Therapeutics. *Nat. Nanotechnol.* **2009**, *4*, 627–633.
- Ménard-Moyon, C.; V. E.; Fabbro, C.; Samori, C.; Da Ros, T.; Kostarelos, K.; Prato, M.; Bianco, A. The Alluring Potential of Functionalized Carbon Nanotubes in Drug Discovery. *Expert Opin. Drug Delivery* **2010**, *5*, 691–707.
- Prato, M.; Kostarelos, K.; Bianco, A. Functionalized Carbon Nanotubes in Drug Design and Discovery. *Acc. Chem. Res.* **2008**, *41*, 60–68.
- Ilbasmis-Tamer, S.; Yilmaz, S.; Banoglu, E.; Degim, I. T. Carbon Nanotubes to Deliver Drug Molecules. *J. Biomed. Nanotechnol.* **2010**, *6*, 20–27.
- Pantarotto, D.; Singh, R.; McCarthy, D.; Erhardt, M.; Briand, J. P.; Prato, M.; Kostarelos, K.; Bianco, A. Functionalized Carbon Nanotubes for Plasmid DNA Gene Delivery. *Angew. Chem. Int. Ed.* **2004**, *43*, 5242–5246.
- Herrero, M. A.; Toma, F. M.; Al-Jamal, K. T.; Kostarelos, K.; Bianco, A.; Da Ros, T.; Bano, F.; Casalis, L.; Scoles, G.; Prato, M. Synthesis and Characterization of a Carbon Nanotube–Dendron Series for Efficient siRNA Delivery. *J. Am. Chem. Soc.* **2009**, *131*, 9843–9848.
- Menard-Moyon, C.; Kostarelos, K.; Prato, M.; Bianco, A. Functionalized Carbon Nanotubes for Probing and Modulating Molecular Functions. *Chem. Biol.* **2010**, *17*, 107–115.
- Luo, P. G.; Wang, H.; Gu, L.; Lu, F.; Lin, Y.; Christensen, K. A.; Yang, S. T.; Sun, Y. P. Selective Interactions of Sugar-Functionalized Single-Walled Carbon Nanotubes with *Bacillus* Spores. *ACS Nano* **2009**, *3*, 3909–3916.
- Wang, H.; Gu, L.; Lin, Y.; Lu, F.; Mezziani, M. J.; Luo, P. G.; Wang, W.; Cao, L.; Sun, Y. P. Unique Aggregation of Anthrax (*Bacillus anthracis*) Spores by Sugar-Coated Single-Walled Carbon Nanotubes. *J. Am. Chem. Soc.* **2006**, *128*, 13364–13365.

36. Elkin, T.; Jiang, X.; Taylor, S.; Lin, Y.; Gu, L.; Yang, H.; Brown, J.; Collins, S.; Sun, Y. P. Immuno-Carbon Nanotubes and Recognition of Pathogens. *ChemBiochem*. **2005**, *6*, 640–643.
37. Gu, L.; Elkin, T.; Jiang, X.; Li, H.; Lin, Y.; Qu, L.; Tzeng, T. R.; Joseph, R.; Sun, Y. P. Single-Walled Carbon Nanotubes Displaying Multivalent Ligands for Capturing Pathogens. *Chem. Commun. (Cambridge)* **2005**, 874–876.
38. O'Shaughnessy, E. M.; Lyman, C. A.; Walsh, T. J. Amphotericin B: Polyene Resistance Mechanisms. In *Antimicrobial Drug Resistance*; Georgiev, V. S., Ed.; Humana Press: Totowa, NJ, 2009; pp 295–305.
39. Canton, E.; Peman, J.; Gobernado, M.; Viudes, A.; Espinel-Ingroff, A. Patterns of Amphotericin B Killing Kinetics against Seven *Candida* Species. *Antimicrob. Agents Chemother.* **2004**, *48*, 2477–2482.
40. Canton, E.; Peman, J.; Sastre, M.; Romero, M.; Espinel-Ingroff, A. Killing Kinetics of Caspofungin, Micafungin, and Amphotericin B against *Candida guilliermondii*. *Antimicrob. Agents Chemother.* **2006**, *50*, 2829–2832.
41. Benincasa, M.; Scocchi, M.; Pacor, S.; Tossi, A.; Nobili, D.; Basaglia, G.; Busetto, M.; Gennaro, R. Fungicidal Activity of Five Cathelicidin Peptides against Clinically Isolated Yeasts. *J. Antimicrob. Chemother.* **2006**, *58*, 950–959.
42. Sokol-Anderson, M. L.; Brajtburg, J.; Medoff, G. Amphotericin B-Induced Oxidative Damage and Killing of *Candida albicans*. *J. Infect. Dis.* **1986**, *154*, 76–83.
43. Escorcia, F. E.; McDevitt, M. R.; Villa, C. H.; Scheinberg, D. A. Targeted Nanomaterials for Radiotherapy. *Nanomedicine* **2007**, *2*, 805–815.
44. Dumortier, H.; Lacotte, S.; Pastorin, G.; Marega, R.; Wu, W.; Bonifazi, D.; Briand, J. P.; Prato, M.; Muller, S.; Bianco, A. Functionalized Carbon Nanotubes Are Non-cytotoxic and Preserve the Functionality of Primary Immune Cells. *Nano Lett.* **2006**, *6*, 1522–1528.
45. Hitchcock, C. A.; Barrett-Bee, K. J.; Russell, N. J. The Lipid Composition and Permeability to Azole of an Azole- and Polyene-Resistant Mutant of *Candida albicans*. *J. Med. Vet. Mycol.* **1987**, *25*, 29–37.
46. Subden, R. E.; Safe, L.; Morris, D. C.; Brown, R. G.; Safe, S. Eburicol, Lichesterol, Ergosterol, and Obtusifolol from Polyene Antibiotic-Resistant Mutants of *Candida albicans*. *Can. J. Microbiol.* **1977**, *23*, 751–754.
47. Ghannoum, M. A.; Rice, L. B. Antifungal Agents: Mode of Action, Mechanisms of Resistance, and Correlation of These Mechanisms with Bacterial Resistance. *Clin. Microbiol. Rev.* **1999**, *12*, 501–517.
48. Vyas, S. P.; Gupta, S. Optimizing Efficacy of Amphotericin B through Nanomodification. *Int. J. Nanomedicine*. **2006**, *1*, 417–432.
49. Liu, Z.; Tabakman, S.; Welsher, K.; Dai, H. Carbon Nanotubes in Biology and Medicine: *In Vitro* and *In Vivo* Detection, Imaging, and Drug Delivery. *Nano Res.* **2009**, *2*, 85–120.
50. Liu, Z.; Davis, C.; Cai, W.; He, L.; Chen, X.; Dai, H. Circulation and Long-Term Fate of Functionalized, Biocompatible Single-Walled Carbon Nanotubes in Mice Probed by Raman Spectroscopy. *Proc. Natl. Acad. Sci. U.S.A.* **2008**, *105*, 1410–1415.
51. Schipper, M. L.; Nakayama-Ratchford, N.; Davis, C. R.; Kam, N. W.; Chu, P.; Liu, Z.; Sun, X.; Dai, H.; Gambhir, S. S. A Pilot Toxicology Study of Single-Walled Carbon Nanotubes in a Small Sample of Mice. *Nat. Nanotechnol.* **2008**, *3*, 216–221.
52. Sayes, C. M.; Liang, F.; Hudson, J. L.; Mendez, J.; Guo, W.; Beach, J. M.; Moore, V. C.; Doyle, C. D.; West, J. L.; Billups, W. E.; *et al.* Functionalization Density Dependence of Single-Walled Carbon Nanotubes Cytotoxicity. *In Vitro. Toxicol. Lett.* **2006**, *161*, 135–142.
53. Cui, D.; Tian, F.; Ozkan, C. S.; Wang, M.; Gao, H. Effect of Single Wall Carbon Nanotubes on Human HEK293 Cells. *Toxicol. Lett.* **2005**, *155*, 73–85.
54. Lam, C. W.; James, J. T.; McCluskey, R.; Hunter, R. L. Pulmonary Toxicity of Single-Wall Carbon Nanotubes in Mice 7 and 90 Days after Intratracheal Instillation. *Toxicol. Sci.* **2004**, *77*, 126–134.
55. Warheit, D. B.; Laurence, B. R.; Reed, K. L.; Roach, D. H.; Reynolds, G. A.; Webb, T. R. Comparative Pulmonary Toxicity Assessment of Single-Wall Carbon Nanotubes in Rats. *Toxicol. Sci.* **2004**, *77*, 117–125.
56. Poland, C. A.; Duffin, R.; Kinloch, I.; Maynard, A.; Wallace, W. A.; Seaton, A.; Stone, V.; Brown, S.; Macnee, W.; Donaldson, K. Carbon Nanotubes Introduced into the Abdominal Cavity of Mice Show Asbestos-like Pathogenicity in a Pilot Study. *Nat. Nanotechnol.* **2008**, *3*, 423–428.